Developmental differentiation in a cytoplasm-dwelling obligate intracellular bacterium

Suparat Giengkam[a], Jantana Wongsantichon[a], Sharanjeet Atwal[b], Yanin Jaiyen[a], Wah Ing Goh[c], Graham D. Wright[c], Taerin, Chung[c], Hyun Huh[c], Sanghyuk Lee[d], Radoslaw M. Sobota[d,g] and Jeanne Salje[a, b, h#]

Mahidol-Oxford Tropical Medicine Research Unit, Faculty of Tropical Medicine, Mahidol University, Bangkok, Thailand[a]

Public Health Research Institute, Rutgers the State University of New Jersey, Newark, USAb

A*STAR Microscopy Platform, Skin Research Institute of Singapore, A*STAR, 8A Biomedical Grove, #06-06 Immunos, Singapore, 138648[c];

Institute of Molecular and Cell Biology, Functional Proteomics Laboratory, Agency for Science, Technology and Research (A*STAR), 138673, Singapore[d]

Institute for Quantitative Biomedicine, Rutgers University, Piscataway, New Jersey 08854, USA[e]

Department of Physics and Astronomy, Rutgers University, Piscataway, New Jersey 08854, USA[f]

Institute of Medical Biology, Agency for Science, Technology and Research (A*STAR), 138648, Singapore[g]

Centre for Tropical Medicine and Global Health, Nuffield Department of Medicine, University of Oxford, Oxford, United Kingdom[h]

[#] Address correspondence to Jeanne Salje: js2522@rutgers.edu

Abstract (150 words)

Developmental differentiation has been described for several vacuole-dwelling obligate intracellular bacteria but never for an obligate intracellular bacterium that resides in the cytoplasm. Here, we show that the cytoplasm-dwelling obligate intracellular bacterium *Orientia tsutsugamushi* (Ot) exists in five distinct subpopulations. We show that Ot differentiates into a distinct, metabolically inactive, extracellular state upon budding from the surface of host cells and that this stage is preceded by a surface-associated maturation stage. We identify proteins that are differentially expressed in intracellular, replicative bacteria and extracellular, metabolically inactive bacteria. Metabolic activity resumes rapidly upon entry into the cytoplasm and is triggered by the host cell reducing environment. This example of developmental differentiation in a species of Rickettsiaceae provides a new model system for studying synchronized differentiation in a bacterium that has a minimal genome and where the interactions between bacterium and host cell are more direct than they are for bacteria separated from the eukaryote cell host by a vacuolar membrane.

Keywords (3-10)

Orientia tsutsugamushi, Rickettsiales, obligate intracellular bacteria, intracellular pathogens, bacterial development.

Author Summary

Scrub typhus is a life-threatening human infection that is caused by the bacterium *Orientia tsutsugamushi* and spread by mites. Although the disease is estimated to affect at least one million people annually and is often fatal, the infectious agent is much less well understood than many other pathogens. *O. tsutsugamushi* is an intracellular bacterium that can only grow and divide within eukaryotic cells. During infection, it is found primarily in the cells that make up the lining of blood vessels and in certain immune cell types. *O. tsutsugamushi* bacteria can remain inside a single infected cell for seven days or more before budding out. The ways in which the bacterium itself changes during the course of an intracellular infection cycle have not been studied. In the current work, we used a range of techniques to show that *O. tsutsugamushi* differentiates into five distinct subpopulations, and that these are associated with measurable differences in metabolic activity, replication and infectivity. This work opens new avenues of research into the regulation and mechanisms of differentiation of *O. tsutsugamushi*, which could lead to improved diagnosis and treatments. It also provides a new model system for studying fundamental questions about bacterial development.

Introduction

Bacteria are commonly thought of as single-celled organisms whose physiology fluctuates in response to environmental changes but that lack the complex differentiation associated with multicellular organisms. Multiple examples now show, however, that bacterial cells can differentiate into morphologically and physiologically distinct subpopulations[1] that coexist within multicellular microcolonies – such as the subpopulations within bacterial biofilms[2] or the differentiation of Streptomyces within hyphae[3] – or that undergo developmentally regulated transitions, for example, into and out of the sporulation state in the cases of *Baccilus subtilis*[4] and *Clostridium difficile*[5]. Transitions between these subpopulations require the bacteria to sense and integrate signals from the environment (including from other bacteria) and to transform this information into physiological and morphological changes by regulating gene expression and protein function. Studying these systems thus reveals fundamental principles about how bacteria sense and respond to their environment as well as how differentiation contributes to fitness and virulence.

Obligate intracellular bacteria depend on their eukaryotic host cells for their growth and division[6]; they have lost genes for free living, including those encoding the components of many metabolic pathways[7]. Consequently, they have streamlined genomes and employ minimal functional systems. For example, whereas the cell division apparatus of the free-living *Escherichia coli* employs 10 Fts proteins, only four of them (FtsA, FtsZ, FtsQ, FtsK) are present in the Rickettsiales *Rickettsia typhi, Wolbachia, Anaplasma marginale* and only one (FtsK) is present in the unrelated obligate intracellular bacterium *Chlamydia*[8]. Obligate intracellular bacteria reside either within membrane-bound vacuoles in the host cell or directly in the host cell cytoplasm. The genomic simplicity of these organisms combined with their intimate relationship with their cellular hosts makes them attractive systems for studying bacterial physiology, host–pathogen biology, and questions about how bacteria sense and

respond to their environment. Obligate intracellular bacteria are difficult to propagate in the laboratory, however, and are mostly genetically intractable[9], thus our understanding of their biology lags behind that of free-living counterparts.

Developmental differentiation has been described for a number of vacuole-dwelling obligate intracellular bacteria, including *Chlamydiales* spp., *Coxiella burnettii, Anaplasma* spp. and *Ehlrichia* spp.[10–18]. In these cases, the bacteria differentiate between a small, non-replicative, infectious extracellular state and a membrane-bound, elongated, replicative intracellular state, which may or may not be infectious depending on the organism. These two populations are easily recognizable under the light microscope due to their differences in size. Such developmental subpopulations have not yet been described in cytoplasm-dwelling obligate intracellular bacteria.

Orientia tsutsugamushi (Ot; order Rickettsiales, family Rickettsiaceae) is a cytoplasm-dwelling obligate intracellular bacterium that causes scrub typhus, one of the most severe rickettsial diseases and the agent of an estimated 1 million human infections each year[19]. The bacterium spreads primarily by the bite of the larval stage of a mite. Bacteria inoculated into the skin replicate in the skin lesion and then disseminate through the lymphatic and circulatory systems[20]. Ot can replicate in a range of cell types including endothelial, epithelial, fibroblast, monocyte/macrophage and dendritic cells[20–23]. If not treated promptly and appropriately, systemic infection can lead to severe complications including multiple organ failure and death. Challenges in achieving rapid and unambiguous diagnosis of scrub typhus[24] means that frequently there are delays in administering appropriate antibiotic therapy; currently, there is no effective human vaccine[25].

Extensive research over the past 20 years has led to the current model for the intracellular infection cycle of Ot. First, the major surface protein of the bacterium, TSA56, interacts with fibronectin, syndecan-4 and integrin α5ß1 on the host cell surface to induce uptake by a clathrin-dependent mechanism[26–29]. The Ot autotransporter surface protein ScaC also functions as an adhesin in this mechanism[30]. Upon entry, Ot escapes into the cytoplasm from LAMP2-containing late endosomes by a pH-dependent mechanism[27]. The cytoplasmic bacteria induce and then escape from autophagy[31,32], and they move to the perinuclear region by a dynein-dependent, microtubule-mediated process[33]. The perinuclear bacteria undergo division by binary fission and remain in a tightly packed microcolony encased in a bacterially derived polysaccharide[34]. Following replication, bacteria move to the cell surface and leave the cell by a virus-like budding process[35] that depends on the bacterial surface protein TSA47 as well as host-derived cholesterol-rich lipid rafts[36]. Extracellular bacteria are unable to replicate by themselves; they must enter new cells to initiate a new round of infection.

Differentiation of Ot into distinct subpopulations during its infection cycle has not been described previously. In our earlier studies, despite careful controls, we encountered a high degree of variation in the growth rate of the bacteria between experiments (unpublished data and also described in ref.[37]). We reasoned that this variation between experiments might be explained by two or more distinct subpopulations of Ot that were able to infect host cells: the infection cycles initiated by bacteria in distinct states might grow differently depending on their distinct protein compositions at the point of infection.

Here, we present evidence that Ot differentiates into five distinct subpopulations, which we term: early entry, pre-replicative, replicative, maturation and extracellular. These are defined in terms of their shape, metabolic activity, DNA replication activity, presence of marker

genes and subcellular location of the bacteria in each subpopulation. This provides a new framework for thinking about the cell biology of Ot and also offers a new model for developmental differentiation in a cytoplasmic dwelling obligate intracellular bacterium. An advantage of studying obligate intracellular bacteria is that they have streamlined genomes and thus the systems involved in sensing the environment, regulating gene expression, bacterial growth and cell division are simplified when compared with those of free-living bacteria. The obligate intracellular lifestyle also imposes synchrony on bacterial populations, whose cellular infection cycle begins again at the point of entry into naïve host cells. As a cytoplasm-residing bacterium, Ot has the added particularity that interactions between the bacterium and host cell are not mediated through a vacuolar membrane.

Results

Ot differentiates into a distinct extracellular state

Cytoplasm-dwelling bacteria including *Rickettsia* spp. generally either spread directly into adjacent cells by means of an actin-propelled mechanism or lyse infected host cells, so releasing the cytoplasmic contents including infectious particles. Ot, by contrast, employs an unusual mechanism to escape from infected host cells. Individual bacteria move to the plasma membrane and bud off the surface by a process reminiscent of the budding of enveloped viruses. An important potential consequence of this budding process is that that the bacterial cells might adopt a dedicated extracellular state. Such an extracellular form of an obligate intracellular bacterium would be expected, by definition, to be metabolically inactive.

To address the question of whether extracellular, budded Ot bacteria exist in a distinct metabolic state from intracellular bacteria, we isolated the extracellular population from the supernatant of infected L929 (mouse fibroblast) cells and the intracellular population by lysing infected host cells. Growth curves of bacterial copy number as determined by qPCR of bacterial DNA showed that the bacterial level in the supernatant began to rise at 4 days post infection (d.p.i.) and increased around one hundred-fold by 6 d.p.i. (Fig. 1A). We therefore compared the intracellular and extracellular populations at 4 d.p.i. and later. At 4 d.p.i., the intracellular and extracellular populations had distinct protein profiles, as determined by shotgun proteomics (Fig. 1B, correlation coefficient = 0.843) suggesting that they were in distinct developmental stages. At 7 d.p.i., by contrast, we saw no difference in the intracellular and extracellular bacteria's protein profiles (Fig. 1B, correlation coefficient = 1), suggesting that by this time the intracellular bacteria had transitioned into a state resembling the extracellular state.

To characterize the morphology of the intracellular and extracellular populations of Ot, we used super-resolution stochastic optical reconstruction microscopy (STORM), with which we

identified two morphotypes: small round bacteria and elongated bacteria (Fig. 1C). A quantitative analysis of confocal microscopy images in the intracellular population showed that the small round cells were prevalent 1–3 hours p.i. (h.p.i.) whereas the elongated form was enriched in populations at 1–7 d.p.i. (Fig. 1D). Thus, in addition to having a distinct protein profile, the extracellular population has a distinct morphology, further supporting the conclusion that the extracellular state of Ot is a distinct developmental state.

To investigate whether both the extracellular and intracellular stages were competent for infection, we isolated both intracellular and extracellular populations 5 d.p.i and measured their ability to infect and grow inside cells by using a qPCR-based analysis. We found that, despite the differences in their protein profiles, both populations were able to infect cells and replicate, although the growth dynamics were slightly different (Fig. 1E). Whilst this result strongly suggests that both populations are infectious, we cannot rule out the possibility that the populations are not completely pure and that residual extracellular bacteria in the intracellular population are responsible for the bacterial growth observed. When we repeated this experiment using extracellular and intracellular populations taken 6 d.p.i. the growth dynamics were more similar (Fig. 1E). This is consistent with our finding that at later time points the protein content of the intracellular and extracellular populations were more similar to one another than they were at 5 d.p.i., reinforcing the notion of temporally regulated development of Ot at the population level.

Ot differentiates into a surface-associated maturation stage

From our conclusion that intracellular and extracellular bacteria are similar to each other at later times of infection, in terms of protein profile and infectivity, whereas they differ at earlier times, we hypothesised that Ot transitions to the extracellular stage by passing through an intracellular maturation stage. To search for these two intracellular populations, we generated an antibody against the Ot autotransporter family outer membrane protein ScaC (Supp. Fig. 1) and used it to identify bacteria in infected L929 cells by immunofluorescence

microscopy. We used a second antibody against a widely expressed surface protein TSA56 to counterstain bacteria, and found that the ScaC antibody labelled only a subpopulation of Ot cells that were located at the surface of infected cells (Fig. 2). Since Ot buds from the plasma membrane of infected cells, we identified this as a potential marker protein for a distinct developmental stage: the maturation stage. The fact that the protein profile of intracellular bacteria at 7 d.p.i is similar to the extracellular bacteria at that time point suggests that these maturation stage bacteria, prevalent at later time points, are in a similar stage as the extracellular stage, although they remain associated with host cells.

Confocal immunofluorescence microscopy of L929 cells infected with Ot and labelled with the antibody against ScaC at 0 and 3 h.p.i. and at 1–7 d.p.i. showed bacteria labelled with ScaC at early time points; this labelling disappeared when intracellular bacteria relocated to the perinuclear region and reappeared in bacteria at the cell surface beginning 3 d.p.i. (Supp. Fig. 2). We repeated the ScaC labelling experiment in the rat kangaroo epithelial cell line Ptk2, which is very flat, so facilitating the imaging. Since growth of Ot has not been shown in this cell line before, we generated a growth curve and found that Ot growth in Ptk2 cells is comparable to that in L929 cells (Supp. Fig. 3). We observed both round and elongated morphologies as for L929-infected Ot, and when we labelled Ot in Ptk2 cells with the antibody against ScaC, we confirmed that not all intracellular bacteria labelled with the antibody and that both surface-associated and extracellular bacteria were labelled (Fig. 2 and Supp. Fig. 4). In contrast to Ot in L929 cells, however, we found that perinuclear bacteria labelled with ScaC from 4 d.p.i onwards. In L929 cells, these intracellular bacteria never labelled with ScaC. This suggests that induction of the maturation stage in Ptk2 cells begins earlier than in L929 cells when bacteria are still located in the perinuclear region. These data confirm the finding that expression of ScaC is regulated in Ot, but indicate that host cell type affects the exact progression of the intracellular infection cycle of Ot.

The extracellular stage of Ot is enriched in proteins involved in dormancy and other processes

We analyzed the proteomic profiles of extracellular and intracellular Ot populations to see whether enrichment of particular proteins would give us clues about the differential activity of these subpopulations and their mechanisms of gene regulation (Tables 1 and 2). We found a significant (>2 fold) upregulation of 60 and 47 proteins in the intracellular and extracellular populations, respectively Three or more of these upregulated proteins were involved in each of the following classes: protein synthesis (20), effectors and secretion (13), energy metabolism (13), DNA binding, repair and replication (6), oxidation-reaction processes (11), lipid and membrane (3), RNA binding and processing (4), transposase (3), dormancy/stringent response/heat stress (3), signaling (3) and peptidoglycan (2) (Fig. 3). This indicated that these classes of proteins may be important in the differentiation into and out of the extracellular state.

Among the proteins upregulated in the extracellular population, notably, three were involved in dormancy/stringent response/heat stress: the (p)pGpp synthetase/hydrolase SpoT (4.99 fold), the alternative heat-response sigma factor RpoH (3.25 fold) and the GTPase ObgE (2.80 fold)[38]. Also, the DNA-binding protein YbaB/EbfC was upregulated 5.02 fold in the extracellular state. The function of this protein in Ot is unknown, however, in the tick-borne bacterium *Borrelia burgdorferei* it is involved in differential DNA compaction during stationary phase and exponential stage growth[39], thus it might play a similar role in Ot.

A number of effector proteins and secretion system proteins were also upregulated in the extracellular and intracellular states: TPR 3 (6.13 fold), TPR 8-1 (4.94 fold) and TPR 8-2 (3.08 fold) in the extracellular state and Ank 1 (12.28 fold), Ank 13-1 (4.90 fold), Ank 13-2 (4.80 fold) in the intracellular state. These proteins belong to two classes of predicted secreted effector proteins in Ot: tetratricopeptide repeat proteins (TPR) and ankyrin repeat

proteins (Ank).This may reflect a need for these proteins for interactions with host cells at different stages of the infection. ScaC was upregulated 1.87 fold in the extracellular population consistent with our immunofluorescence microscopy data.

Ot resumes metabolic activity shortly after entry into host cells

Following their entry into host cells, there is a lag of 24–48 hours before replication of Ot can be detected[40]. To investigate whether the metabolic activity of the bacteria is subject to a similar lag following infection, we devised a single cell microscopy assay in which we identified metabolically active bacteria based on their ability to incorporate a methionine derivative into nascent proteins as a measure of metabolic activity[41] and used click chemistry to measure the incorporation. The 'clickable' methionine-alkyne derivative (homopropyl serine HPG) was added to the growth medium for 30 minutes prior to fixation of the infected cells, it was then reacted with an azide-fluorophore in a copper-catalyzed click reaction. The metabolically active bacteria were identified by their green fluorescence, and the intensity of the fluorescence provided a measure of the amount of translation. The bacterial signal after 30 minutes incubation was sufficiently strong to be detected easily against the host cell background.

We used this HPG incorporation assay to measure the metabolic activity of Ot throughout the infection cycle (Fig. 4). In contrast to the lag in DNA replication, protein synthesis was routinely detected as early as 1 h.p.i., demonstrating that Ot is primed to resume metabolic activity upon entry into host cells. This observation allowed us to define three more steps in the infection cycle of Ot: the early entry stage describes Ot that has entered host cells but is not yet metabolically active; the pre-replicative stage describes Ot that is metabolically active but that has not yet initiated DNA replication, and the replicative stage describes Ot that is undergoing metabolic activity and DNA replication. Inspection of the complete time course revealed that surface-associated Ot – the maturation stage – retains metabolic activity (Fig.

4 and Supp. Fig 5). Metabolic activity ceases only when the bacteria have left the cells. We observed that extracellular bacteria could never be labelled with HPG, consistent with a complete absence of protein synthesis in this state. Equivalent clickable probes are available to study DNA and RNA synthesis by using nucleotide analogues[42], but we were unable to obtain labelling of Ot with these probes under any conditions even though the host cells were clearly labelled. This may reflect an inability of this bacterium to take up these modified nucleotides.

Ot is internalized into host cells by a clathrin-mediated endocytic mechanism[27]. The bacteria then progress through the endocytic pathway before escaping from late endosomes into the cytoplasm. Given the early initiation of metabolic activity, we asked whether Ot is active within the endosomes or only upon exit into the cytosol. To address this question, we isolated intracellular and extracellular bacteria from host cells 5 d.p.i. and used them to infect host cells. We added the clickable methionine analog HPG to the growth medium for 15–30 mins, then fixed samples of the cells at 15 mins, 30 mins, 1 hour or 24 h.p.i. and labelled the cells with an antibody against the late endosome marker LAMP1, a 16S RNA FISH probe specific for Ot, and with a fluorescent azide that reacts with HPG (Fig. 5A). The majority of bacteria were either LAMP1-positive or HPG-positive (Fig. 5A and quantified in 5B) indicating that the bacteria in endosomes were metabolically inactive and cytoplasmic bacteria were metabolically active. A small proportion of bacteria (2–10%) at 30 min and 1 h.p.i. were labelled with both LAMP1 and HPG (Fig. 5B). These may be bacteria in intact endosomes or in endosomes in the process of lysing. To demonstrate that bacteria inside intact endosomes could be labelled with HPG if they were metabolically active, we labelled intracellular *Salmonella typhimurium,* which remains within membrane-bound endosomes (Supp. Fig. 6). Thus, these data indicate that Ot broadly initiates protein synthesis upon its exit from endosomes into the cytoplasm. A comparison of the magnitude and timing of this activation between intracellular and extracellular bacteria indicated that extracellular bacteria

escaped endosomes slightly faster than the intracellular bacteria (Fig. 5B). These differences were small, however; a detailed investigation of the differences between these populations in early stages of infection will require more sensitive assays.

Bacterial activation is triggered by the reducing environment of the host cell cytoplasm

The observation that bacteria mostly initiate protein synthesis upon exposure to the cytoplasm raised the question: what triggers the resumption of metabolic activity in intracellular Ot? We have previously shown that the bacterial outer membrane protein TSA56 forms a disulfide crosslinked network[43]. We hypothesized that this, and potentially other proteins containing exposed Cys residues, might become reduced upon exposure to the reducing environment of the host cell cytoplasm and that this might trigger an internal signal to activate metabolism. To test this, we used the drug buthionine sulfoximine (BSO) that decreases the levels of reduced glutathione in mammalian cells, making the cytoplasm less strongly reducing. This drug did not affect the ability of Ot to infect cells (Supp. Fig. 7), however, it significantly reduced the intensity of HPG staining in a dose-dependent way at 1, 2 and 24 h.p.i. (Fig. 5C). This demonstrated that the reducing environment plays a role in the reactivation of Ot upon entry into host cells.

Ot regulates its gene expression during the intracellular stages of infection

The data described above show that intracellular Ot differentiates into distinct subpopulations that can be resolved by microscopy based on their metabolic activity, subcellular localization, cell shape and expression of the marker protein ScaC. This differentiation is likely driven by changes in gene expression. To gain an overview of which genes may be differentially expressed in the distinct subpopulations, we isolated the RNA from intracellular bacteria 1, 3, 5 and 7 d.p.i. and analyzed gene expression by qRT-PCR using primers for genes encoding surface proteins and proteins involved in cell wall

biogenesis (Supp. Fig. 8). Whereas the expression of some genes remained constant (*murF, scaD, scaE*), others increased (*scaA, tsa47, tsa56*) or decreased (*pbp2, ddl, murA, murD, tsa22, pal*) over the course of a 7-day infection. Despite the limitation that this approach averages together data from different subpopulations within one time point, the data demonstrate that Ot undergoes regulated transitions in gene expression over the course of its life cycle.

Discussion

Here, we show that Ot differentiates into distinct subpopulations over the course of a 5–7-day infection of a host cell and that this culminates in the release from the cell of bacteria that are in a different state (stage V) from those inside the cell (stages I–IV) (Fig. 6). This has parallels with the biphasic lifecycle of *Chlamydia* spp., which include common human pathogens, and some Anaplasmataceae, which include vector-borne human and animal pathogens; however, no similar phenomenon has been described for any other Rickettsiaceae family member. *Orientia* is the only genus of the Rickettsiaceae reported to exit infected cells by budding off from the cell surface into the extracellular space rather than moving directly into adjacent cells. Membrane-bound extracellular bacteria can infect cells and may be important for systemic dissemination during infection. This unique aspect of the infection cycle may explain why *Orientia* undergoes differentiation into specific developmental stages.

Orientia is also the only genus in the Rickettsiaceae that encodes a full-length gene for SpoT, in addition to the multiple truncated SpoT genes that are found in other Rickettsiaceae. SpoT encodes a bifunctional enzyme that synthesizes and hydrolyses (p)ppGpp, a small molecule typically induced during starvation or stress that regulates the induction of multiple stress-response genes. The finding that SpoT is upregulated in the extracellular stage (V) of Ot when compared with the intracellular stage (III) suggests a

possible role for SpoT-regulated (p)ppGpp synthesis in regulating the transition into stages IV and V in response to nutrient limitation in highly infected host cells.

The specific expression of ScaC on surface-residing bacteria and the differential protein profiles of intracellular and extracellular bacteria, demonstrate that Ot transitions into a distinct, developmentally regulated state prior to exit rather than simply terminating metabolic activity in response to the sudden absence of nutrients when the bacteria are released from the host cell. This extracellular stage (stage V) is likely to be similar to the stationary phase in free-living bacteria, and the genes enriched in this population will be required both for transitioning into this state and also priming it for reactivation upon infection into new cells. The enrichment of peptidoglycan-related gene products (MurC, MurE) in the proteomics analysis and the finding from qRT-PCR that peptidoglycan biosynthesis genes (*pbo2, ddl, murA, pal, murD*) are upregulated early during infection suggests that cell wall synthesis is an important process in early stages of intracellular growth. Other proteins enriched in the extracellular stage included four TPR proteins (TPR-3 and TPR8-1, TPR8-2, TPR8-3*). ank and tpr* genes are present in multiple copies in the genome of Ot[44] and their protein products have been shown to be exported as effector proteins with multiple target locations and functions[45–48]. Based on their presence in extracellular stage Ot, these particular TPR proteins may play a role in early stages of bacterial infection. By contrast, the intracellular (stage III) bacteria expressed high levels of Ank1, Ank13-1 and Ank13-2, suggesting a role for these effector proteins in subverting later host defenses against bacterial replication.

The presence of high levels of ScaC on maturation stage (IV) and extracellular stage (V) bacteria is consistent with a role for ScaC in adhesion and entry[30]. No additional role for ScaC in budding out of host cells is known. ScaC is lost from the bacterial surface shortly after infection. This may be due to targeted degradation or secretion of the protein into host cells. Ot has been shown to shed outer membrane vesicle (OMV)s, so ScaC may be

secreted in this way. The surface protein TSA56 did not show the same expression patterns as ScaC (Fig. 2A), however, so shedding of ScaC in OMVs would have to be protein specific. Alternatively, the levels of TSA56 might be so high that a loss through OMV shedding might not be apparent. ScaC, a protein of the autotransporter family, contains a ß-barrel and an extracellular autotransporter domain, which is sometimes cleaved in other proteins of this family. Our ScaC antibody targets an epitope on the autotransporter domain, therefore, it is possible that a loss of labelling results from cleavage of this domain and its release into the host cell cytoplasm.

The mechanisms regulating the expression of maturation/extracellular stage genes are unknown, as are the triggers that activate the transition into stages IV and V. Ot encodes two main translation initiation factors (sigma factors), RpoD and RpoH, as well as RpsD, which was shown to be a sigma factor in *Chlamydia trachomatis*[49]. We found that RpoH, which was initially described as a heat shock response regulator but has since been shown to regulate the response to other stresses too[50], was upregulated in the extracellular stage (V) suggesting that this may coordinate the upregulation of multiple extracellular stage genes. Ot encodes only 12 predicted transcription factors, however, indicating that other mechanisms that regulate gene expression may be important. Consistent with this, ribosomal accessory proteins RplX and RbfA (50S ribosomal protein L24 and ribosome-binding factor A) were both enriched in extracellular bacteria. These proteins are involved in ribosome assembly and may be important for regulating ribosome inactivation and reactivation during dormancy.

The intracellular population of Ot (stages II–IV) comprises metabolically active bacteria undergoing protein synthesis and, in stages III and IV, DNA replication. Of the 15 proteins highly enriched in the intracellular fraction, four are involved in protein synthesis, likely reflecting a general increase in translation and metabolic activity. In addition, three of the 15 proteins are involved in oxidation–reduction processes. The host cell cytoplasm is a more

reducing environment than the extracellular environment. The major surface protein TSA56 of Ot contains three Cys residues and their cross-linking is required for the bacteria to enter host cells[43]. We found that the reducing environment of the host cell cytoplasm is required for activation of metabolic activity upon entry into host cells, as was previously shown for another intracellular bacterium *Listeria monocytogenes*[51,52]. It is possible that other factors such as nutrient availability and pH also play a role in the activation of Ot upon entry into host cells and the study of this as well as the bacterial mechanisms for sensing these environmental triggers will be an area of future study.

Morphological analysis of Ot at different stages of the infection cycle showed that the bacteria change shape over time. Ot is typically described as a coccoid bacterium of 1–2 µm in length. Our data show that the shape of Ot is more varied than this, with both round and elongated morphologies and lengths up to 5 µm. Multiple septa were not observed in these elongated cells, suggesting that they are one long cell rather than a chain of short cells, although the number of nucleoids in one elongated cell has not been measured. The mechanism of length control in Ot is unknown. Highly elongated cells of *R. typhi* growing in a tick cell line have been reported[53] suggesting the possibility that mechanisms for producing different cell morphologies under different conditions may be widespread across the Rickettsiaceae, The morphology of growing Ot, and possibly other rickettsia, may reflect nutrient availability under different conditions. The observation that elongated Ot cells are rod shaped rather than spherical supports the recent finding that Ot synthesizes a peptidoglycan-like structure, although this is not very abundant[43].

We found that both extracellular and intracellular populations of Ot are infectious. This contrasts with some other (vacuole-dwelling) bacteria with a biphasic lifecycle in which only the extracellular population is competent for infection, as well as with other (cytoplasm-dwelling) Rickettsiaceae that pass directly into adjacent cells and are not known to have a dedicated extracellular stage[54]. Direct cell-to-cell transfer of Ot has not been described, but

the fact that intracellular Ot is infectious suggests that this mode of dissemination may exist in parallel to known dissemination via the extracellular route. Both might be important during infection, with cell-to-cell transfer mediating local dissemination and extracellular bacteria mediating systemic dissemination.

Previously, we found a large degree of variation between different experiments in the timing of initiation of DNA replication following entry into host cells as well as the timing of intracellular relocation and bacterial elongation, despite our attempts to standardize conditions. We speculate now that this may have been due to inadvertent mixing of different subpopulations, for example if these populations vary in their timings of metabolic reactivation following host cell entry and bacterial DNA replication. Our findings suggest that future studies should take care to isolate specific populations prior to infections.

The finding that Ot differentiates into distinct subpopulations, and the identification of specific marker genes and proteins associated with these stages, leads to a number of important questions. First, how is the transition between these different stages regulated? For example, what bacteria and host factors are important, and is the time after infection or the copy number of intracellular bacteria important? Second, are the different bacterial stages affected by the bacterial strain and host cell type? For example, how does the transition between different developmental stages affect virulence in clinically important strains of Ot? Finally, how does infection by extracellular and intracellular stage bacteria differ and what is the mechanistic basis of these differences? The current work is the first step in describing bacterial differentiation in Ot and will lead to these and other exciting avenues of research into this important human pathogen.

Methods

Bacterial propagation and quantification

All experiments were performed using the mouse fibroblast cell line L929 (ATCC CCL-1) which was a kind gift from Dr. Blacksell at the Mahidol Oxford Tropical Medicine Research Unit, Bangkok, Thailand, Potoroo kidney Ptk2 cells (Sigma Aldridge 88031601), and the Karp-like clinical isolate strain of *Orientia tsutsugamushi* UT76[40]. Cell culture was performed using DMEM media (L929) or EMEM (Ptk2) with 10 % FBS at 37 ?C (uninfected cells) or 35 ?C (infected cells) and 5% CO_2. For routine propagation bacteria were grown in 25 or 75 cm^2 culture flasks as described previously[40]. Unless otherwise specified experiments were performed using bacteria harvested from the intracellular fraction of infected cells, 7 days after infection.

Fluorescence microscopy

Immunofluorescence labelling and confocal microscopy. All fixed cells were permeabilized in 0.5% TritonX for 15-20 min on ice and incubated in blocking buffer (1XPBS, pH7.4 with 1 mg/ml BSA or 1XPBS, pH 7.4 with blocking using serum from host species of the labeled antibody diluted to 1:20) for 15-20 min at room temperature. Primary antibodies were added for 1 hour at 37 ºC (in house antibodies: rat monoclonal antibody against TSA56 diluted 1:200, rabbit polyclonal antibody against Ot ScaC, commercial antibodies: LAMP1 (Thermo Scientific monoclonal mouse MA1-164 diluted 1:200). Samples were washed 2x with PBS-BSA then the appropriate secondary antibodies were diluted 1:1000 and incubated for 30 mins at 37 ºC in the dark (goat anti-mouse IgG superclonal Alexa Fluor 647 conjugate, Thermo Fisher A28180; goat anti-rat Alexa Fluor 488, Thermo Fisher, A11006; goat anti-rabbit, Alexa Fluor 594, Thermo Fisher A11012) The nuclear stain Hoechst was diluted to 1:1000 and included with the secondary antibody incubation. Phalloidin Alexa Fluor 594 (ThermoFisher Scientific) was used to detect host actin at dilution 1:40. Before add mounting

media (20mM Tris, pH 8.0; 0.5% N-propyl-gallate; 90% glycerol), cells were washed with 1X PBS again. Imaging was performed using a Zeiss Observer Z1 LSM700 confocal microscope with HBO 100 illuminating system, equipped with a 63x/1.4 Plan-APOCHROMAT objective lens (Carl Zeiss, Germany) and 405 nm, 488 nm and 555 nm laser lines, and a Leica TCS SP8 confocal microscope (Leica Microsystems, Germany) equipped with a 63x/1.4 Plan-APOCHROMAT oil objective lens with 1.4 mm working distance, and 405 nm, 488 nm, 552 nm and 638 nm laser lines.

Fluorescence intensity measurements were done manually using Fiji ImageJ software [55]. 30 (Fig. 5B) or 100 (Fig. 5C) individual bacteria were quantified by measuring the brightest pixel intensity within the area of the bacterium. Images within one experiment were acquired under identical laser intensity and image acquisition conditions. Length and width measurements were done manually using Fiji Image J software [55].

STORM imaging and analysis

We acquired 3D-STORM data using a homebuilt multi-color Total Internal Reflection Fluorescence (TIRF) microscope[56] that is based on an inverted microscope (Nikon, Ti-E), a high NA objective (Nikon, CFI-Apo 100X, NA 1.49), a 405 nm photoactivation laser (Coherent, OBIS 405 LX 100mW), a 488 nm excitation laser (MPB, 2RU-VFL-P-20000642-B1R), and an EMCCD camera (Andor, iXon Ultra-888). Samples immunolabelled with Alexa 488 were mounted on the microscope, transferred to STORM buffer (OxyFluor (Oxyrase), 50mM BME (Sigma), 2.5mM COT (Sigma)), and illuminated with strong 488 nm laser to record single-molecule fluorescence blinking events at 25 Hz frame rate. 405 nm illumination was intercalated with pulsed 488nm excitation to enhance photoactivation of Alexa 488 without exacerbating background signal. A cylindrical lens (Thorlabs, LJ1516RM-A) was placed in front of camera in order to determine the z-coordinates of fluorescent molecules through the elongated point spread function (PSF) methods [57]. Each STORM image was reconstructed from single-molecule localization data obtained by the analysis of 30,000 frames with custom Matlab codes. Briefly, bright single fluorescence spots were identified by

thresholding methods, and their 3-D coordinates were determined by 2-D elliptical Gaussian fitting along with a pre-calibrated conversion table between eccentricity and z-coordinate. Focus drift was actively stabilized with Perfect Focus System (Nikon) while acquiring the data, whereas xy-drift was post-corrected using redundant cross-correlation algorithm [58]. Each localization event was represented as a 2-D Gaussian of 20 nm standard deviation in STORM images. For the analysis of bacteria morphology, we picked cells that showed clear cell boundary, manually adjusted the z-coordinate to find the cell midplane, and measured the length of long and short axes.

Click labelling. The metabolic click-labelling is based on the Click-iT HPG Alexa Fluor protein Synthesis Assay Kits (Molecular Probe by Life Technologies). To incorporate L-homopropargylglycine (HPG) at each time point, infected cells were incubated in minimal medium without L-methionine (Dulbecco's Modified Eagle Medium, DMEM, Cat. no. 21013) containing 25 µM HPG for 30 min at 37 ºC. Labelled bacteria were washed twice in PBS + 1mg/ml BSA before fixing with 4% formaldehyde and subsequently permeabilized with 0.5% Triton-X for 20 min on ice. After washing with PBS + 1 mg/ml BSA, Click-iT reaction cocktail was incubated with cells for 30 min at room temperature protected from light. The component of Click-iT reaction cocktail is based on Click-iT HPG Alexa Fluor Protein Synthesis Assay Kits cat. C10428. The Azide dye (Alexa Fluor 488) was used at a final concentration of 5 µM. After click reaction, the cells were ready for immunofluorescent fluorescence labelling and imaging as above.

RNA FISH. The RNA FISH protocol was modified from the protocol described in ref[59]. A confluent monolayer of host cells (L929) were grown in chambered coverslips (Ibidi, USA) for 2 days before infection with different strains of *Orientia tsutsugamushi* at MOI 100:1. These infected cells were washed twice with 1X PBS pH 7.4 before fixing with 4% formaldehyde in 1X PBS for 10 minutes at room temperature, followed by washing with PBS

twice and incubation in 70% ethanol for 1 hour on ice. Cells were further permeabilized with 0.5% triton for 15-20 min on ice, washed with PBS 1X, and incubated with 1mg/ml lysozyme for 1 hour at room temperature. These samples were stained using immunofluorescence (see section above) and then labelled for RNA FISH. For RNA FISH labelling, cells were fixed again with 4% formaldehyde in 1X PBS for 10 minutes at room temperature to stabilize the immunofluorescence signal. Then samples were equilibrated in washing buffer (2X SSC +10% formamide) at room temperature for 5-10 min before hybridization. An in-house RNA-FISH probe was designed against *O. tsutsugamushi 16s* gene and labeled with TexasRed. The probe was resuspended in hybridization buffer (10% Dextran sulfate (w/v) (Sigma, D8906), 1 mg/ml Escherichia coli tRNA (Sigma, R8759), 2 mM Vanadyl ribonucleoside complex (New England Biolab, Ipswich, MA, Catalogue Number, S142), 0.02% RNase free BSA (Ambion, AM2618), 10% formamide) and used at a final concentration of 2 ng/µl. Samples were pre-incubated with the probe at 50 ºC for 3-4 hours and further incubated at 37 ºC for 18-24 hours in the dark. Cells were then washed with washing buffer twice for 10 min at RT in the dark prior to imaging under a confocal microscope.

555555

Gene expression analysis by RT-qPCR

Infected cells were harvested at each time point and were kept in RNAProtect Bacteria Reagent (Qiagen, catalog number 76506) at -80 °C prior to use. Total RNA was extracted using the Qiagen RNeasy Plus kit (Qiagen, catalog number 74136) according to manufacturer's instructions. 10 µg of each total RNA sample was treated with DNaseI (Thermo Fisher Scientific, catalog number AM2238) at 37 °C for 30–60 min before cDNA synthesis using the iScript reverse transcription supermix (Biorad, catalog number 170–8841) with random primers. cDNA was subsequently verified to be free of genomic DNA contamination by using a reverse transcriptase-free control reaction. No PCR products were detected, demonstrating an absence of DNA contamination in RNA samples. cDNA was then used as a template for qPCR using gene-specific primers for *TSA22*, *TSA47*, *TSA56*,

ScaA, *ScaE*, *ScaD*, *murA*, *murD*, *murF*, *ddl* and *pbp2*. RT-qPCR was performed using SYBR green qPCR mix (Biotools, Houston, USA, catalog number 10.609). All the expression levels were normalised relative to the housekeeping gene *mipZ*.

Primer name	Primer sequences (5' to 3')
TSA22_FW	TGGGTGTAGCTGCAGGCATAC
TSA22_RV	GTTGATACACTAGCTGAAGATGAT G
TSA47 forward	TCCAGAATTAAATGAGAATTTAGGAC
TSA47 reverse	TTAGTAATTACATCTCCAGGAGCAA
TSA56 forward	TGCCCAACAAGAAGAAGATG
TSA56 reverse	TTTAACTTGGCCGACAATCA
ScaA forward	ACCGCATTCAAACAGTGATCT
ScaA reverse	CAGTTTTTCCGCCATGAGTTG
ScaD forward	GAGCGACTACGAATGCATCA
ScaD reverse	CAGTTGCATCGTTGTTTTGG
ScaE forward	AGACCACGCAGTAACATGCTT
ScaE reverse	ACTGCGCGCCATTGTTGATT
murA forward	AACGCATGCATCACTTAGACC
murA reverse	CAGGAATTCTTTGGACTCTTGC
murD forward	GCTGGAGGAGTTGCTAAAGAAG
murD reverse	CCCACTTTGATCAGATTCAGC
murF forward	GCCGGTTGATCAGTTGTTG
murF reverse	TTCGATGACTTGCCAAAGC
ddl forward	GGAGAGGATGGATGTATTCCTG
ddl reverse	TATCAAATGCAGCAGCAGAAGT
pbpA2 forward	CGCCTACCCAACATAAACAAG
pbpA2 reverse	TCCTGCTAAACCACGCATATC

mipZ forward	GTGGTGCAGGTAAGACTACTGTTG
mipZ reverse	GTGAATGCTGACGTGAATCAG

Proteomics sample preparation and analysis

Orientia tsutsugamushi strain UT76 was used to infect the mouse fibroblast cell line L929 at MOI 10:1 and 50:1. L929 cells were grown in 75 cm^2 plastic flasks at 37°C and 5% CO_2, using DMEM media supplemented with 10% FBS. Intracellular bacteria were isolated from L929 cells at 3, 5, and 7 days after infection and purified as described previously [40]. Extracellular bacteria were collected from DMEM media by centrifugation at the same time points. Harvested bacteria were then washed with 0.3 M sucrose three times, resuspended in PBS buffer, and lysed with 1% Triton-X at 4?C for 30 minutes. Bacterial proteins were precipitated in 80% ice-cold acetone at -20?C overnight and pelleted by centrifugation at 13,000 x g for 10 minutes. Briefly dried protein pellets were dissolved in 50% trifluoroethanol in 100 mM TEAB buffer. The samples were reduced with 20 mM TCEP and alkylated using 55 mM CAA. Proteins were digested using LysC (1:50 of LysC:protein) at 37?C for 4 hours and then digested with trypsin (1:100 of trypsin:protein) at 37?C overnight. Samples were acidified with TFA to 1% final concentration and centrifuged to remove any precipitant. Samples were desalted using Waters HLB in 96 well plate format. Briefly, following activation with 500 µl of 100% acetonitrile and equilibration with 500 µl of 0.5% acetic acid, samples were passed through the plate, selected wells were washed with 500 µl of MS grade water, and peptide mixtures were eluted with 800 µl of 80% acetonitrile in 100 mM TEAB buffer.

In preliminary runs, 20 µl of each peptide mixtures (2.5% total volume) were dried in a speedvac and the pellets were resuspended in 15 µl of 100 mM TEAB. There were 2 sets of samples – one from MOI 10:1 and the other from MOI 50:1. Each set contains 6 samples including ExtD3, IntD3, ExtD5, IntD5, ExtD7, and IntD7. Selected isobaric TMT tags of TMT10-126, TMT10-127N, TMT10-128C, TMT10-129N, TMT10-130C, and TMT10-131

(Thermo Fisher Scientific, USA) were added to respective sample at 10 µl per tube. Reactions were left at room temperature for 1 hour. For each MOI set, amount of 2 µl were taken from each labeled samples and added into 50 µl of 10 mM ammonium formate pH 10 to a total volume of 62 µl per set. The 2 sets of pooled samples were desalted through high pH C18 reverse phase material stage tips (C-18 ReproSil-Pur Basic, Dr. Maisch, 10µm). Briefly, C18 desalting tips were equilibrated with 50 µl of 100% acetonitrile and followed with 50 µl of 10 mM ammonium formate pH 10 (Solution A). The pooled samples in solution A were loaded onto equilibrated C18 tips, the tips were then washed with 80 µl of solution A, and eluted with 50 µl of 10 mM ammonium formate in 50% acetonitrile (Solution B.) Finally, both sample elutions were completely vacuum dried and pellets were resuspended with 5 µl of [0.5% acetic acid, 0.06% trifluoroacetic acid, 1% acetonitrile] for LC-MS/MS. Protein frequency distributions from preliminary runs were used to normalized sample loadings in actual experiments thereafter.

LC-MS/MS and data analysis

Samples were separated in 120 min gradient (0.1% formic acid in water and 99.9% acetonitrile with 0.1% Formic Acid) on 50 cm x 75 um id Easy-Spray RP column (C-18, 2 µm particles, Thermo) using Easy nLC1000 (Thermo) chromatography system coupled online with Orbitrap Fusion mass spectrometer (Thermo). Data dependent mode was used in a time loop mode -3 s cycle using Orbitrap analyzer for both scans with following ion targets and resolutions (OT-MS 4xE5 ions, resolution 60K, OT-MS/MS 8E4 ions, resolution 15k).

Peak lists were generated using Proteome Discoverer 2.2 software (Thermo). Searches were done with Mascot 2.6.1 (Matrix Science) against forward/decoy Mouse Uniprot and Orientia UT76 database with following parameters: precursor mass tolerance (MS) 20ppm, OT-MS/MS 0.06 Da, 3 miscleavages; Static modifications: carboamidomethyl (C), TMT6plex. Variable modifications: Acetyl N-terminal, oxidation (M), deamidation (NQ),. Forward/decoy searches were used for false discovery rate estimation on peptide and PSM level (FDR 1% high confidence FDR 5% medium confidence).

Acknowledgements and Funding

We thank all the members of the lab for discussions and support. We are grateful to the following people for providing helpful feedback and insights on the project and the manuscript: Jonathan Dworkin from Columbia University, Dave Dubnau from PHRI, Karen Edelblum from Rutgers University, Carol Featherstone from Life Science Editors.

JS was funded by a Royal Society Dorothy Hodgkin Research Fellowship. YJ was funded by a Newton Fund MRC-NSTDA grant. RMS, WIG and GDW are funded by the Agency for Science, Technology and Research (A*STAR) core funding and the NRF Shared Infrastructure Support grant for the Singapore National Laboratory for Mass Spectrometry - *SingMass* (RMS) and *SingaScope* – a Singapore-wide microscopy infrastructure network (WIG and GDW).

References

1. Justice, S. S., Harrison, A., Becknell, B. & Mason, K. M. Bacterial differentiation, development, and disease: mechanisms for survival. *FEMS Microbiol Lett* 360, 1-8 (2014).
2. Kostakioti, M., Hadjifrangiskou, M. & Hultgren, S. J. Bacterial biofilms: development, dispersal, and therapeutic strategies in the dawn of the postantibiotic era. *Cold Spring Harb Perspect Med* 3, a010306 (2013).
3. Chater, K. F. Recent advances in understanding *Streptomyces*. *F1000Res* 5, 2795 (2016).
4. Higgins, D. & Dworkin, J. Recent progress in Bacillus subtilis sporulation. *FEMS Microbiol Rev* 36, 131-148 (2012).
5. Zhu, D., Sorg, J. A. & Sun, X. *Clostridioides difficile* biology: sporulation, germination and corresponding therapies for *C. difficile* infection. *Front Cell Infect Microbiol* 8, 29 (2018).
6. Fields, K. A., Heinzen, R. A. & Carabeo, R. The obligate intracellular lifestyle. *Front Microbiol* 2, 99 (2011).
7. Zientz, E., Dandekar, T. & Gross, R. Metabolic interdependence of obligate intracellular bacteria and their insect hosts. *Microbiol Mol Biol Rev* 68, 745-770 (2004).
8. Otten, C., Brilli, M., Vollmer, W., Viollier, P. H. & Salje, J. Peptidoglycan in obligate intracellular bacteria. *Mol Microbiol* 107, 142-163 (2018).
9. McClure, E. E., Chávez, A. S. O., Shaw, D. K., Carlyon, J. A., Ganta, R. R., Noh, S. M., Wood, D. O., Bavoil, P. M., Brayton, K. A., Martinez, J. J., McBride, J. W., Valdivia, R. H., Munderloh, U. G. & Pedra, J. H. F. Engineering of obligate intracellular bacteria: progress, challenges and paradigms. *Nat Rev Microbiol* (2017).
10. Carlyon, J. A. & Fikrig, E. Invasion and survival strategies of Anaplasma phagocytophilum. *Cell Microbiol* 5, 743-754 (2003).
11. Rikihisa, Y. Anaplasma phagocytophilum and Ehrlichia chaffeensis: subversive manipulators of host cells. *Nat Rev Microbiol* 8, 328-339 (2010).
12. Minnick, M. F. & Raghavan, R. Developmental biology of Coxiella burnetii. *Adv Exp Med Biol* 984, 231-248 (2012).
13. Truchan, H. K., Seidman, D. & Carlyon, J. A. Breaking in and grabbing a meal: Anaplasma phagocytophilum cellular invasion, nutrient acquisition, and promising tools for their study. *Microbes Infect* (2013).
14. van Schaik, E. J., Chen, C., Mertens, K., Weber, M. M. & Samuel, J. E. Molecular pathogenesis of the obligate intracellular bacterium Coxiella burnetii. *Nat Rev Microbiol* 11, 561-573 (2013).
15. Moumène, A. & Meyer, D. F. Ehrlichia's molecular tricks to manipulate their host cells. *Microbes Infect* (2015).
16. Elwell, C., Mirrashidi, K. & Engel, J. Chlamydia cell biology and pathogenesis. *Nat Rev Microbiol* 14, 385-400 (2016).
17. Cossé, M. M., Hayward, R. D. & Subtil, A. One Face of Chlamydia trachomatis: The Infectious Elementary Body. *Curr Top Microbiol Immunol* (2016).
18. König, L., Siegl, A., Penz, T., Haider, S., Wentrup, C., Polzin, J., Mann, E., Schmitz-Esser, S., Domman, D. & Horn, M. Biphasic Metabolism and Host Interaction of a Chlamydial Symbiont. *mSystems* 2, (2017).
19. Watt, G. & Parola, P. Scrub typhus and tropical rickettsioses. *Curr Opin Infect Dis* 16, 429-436 (2003).
20. Paris, D. H., Phetsouvanh, R., Tanganuchitcharnchai, A., Jones, M., Jenjaroen, K., Vongsouvath, M., Ferguson, D. P., Blacksell, S. D., Newton, P. N., Day, N. P. & Turner, G. D. Orientia tsutsugamushi in human scrub typhus eschars shows tropism for dendritic cells and monocytes rather than endothelium. *PLoS Negl Trop Dis* 6, e1466 (2012).

21. Moron, C. G., Popov, V. L., Feng, H. M., Wear, D. & Walker, D. H. Identification of the target cells of Orientia tsutsugamushi in human cases of scrub typhus. *Mod Pathol* 14, 752-759 (2001).
22. Tantibhedhyangkul, W., Prachason, T., Waywa, D., El Filali, A., Ghigo, E., Thongnoppakhun, W., Raoult, D., Suputtamongkol, Y., Capo, C., Limwongse, C. & Mege, J. L. Orientia tsutsugamushi stimulates an original gene expression program in monocytes: relationship with gene expression in patients with scrub typhus. *PLoS Negl Trop Dis* 5, e1028 (2011).
23. Chu, H., Park, S. M., Cheon, I. S., Park, M. Y., Shim, B. S., Gil, B. C., Jeung, W. H., Hwang, K. J., Song, K. D., Hong, K. J., Song, M., Jeong, H. J., Han, S. H. & Yun, C. H. Orientia tsutsugamushi infection induces CD4+ T cell activation via human dendritic cell activity. *J Microbiol Biotechnol* (2013).
24. Saraswati, K., Day, N. P. J., Mukaka, M. & Blacksell, S. D. Scrub typhus point-of-care testing: A systematic review and meta-analysis. *PLoS Negl Trop Dis* 12, e0006330 (2018).
25. Valbuena, G. & Walker, D. H. Approaches to vaccines against Orientia tsutsugamushi. *Front Cell Infect Microbiol* 2, 170 (2012).
26. Kim, H. R., Choi, M. S. & Kim, I. S. Role of Syndecan-4 in the cellular invasion of Orientia tsutsugamushi. *Microb Pathog* 36, 219-225 (2004).
27. Chu, H., Lee, J. H., Han, S. H., Kim, S. Y., Cho, N. H., Kim, I. S. & Choi, M. S. Exploitation of the endocytic pathway by Orientia tsutsugamushi in nonprofessional phagocytes. *Infect Immun* 74, 4246-4253 (2006).
28. Lee, J. H., Cho, N. H., Kim, S. Y., Bang, S. Y., Chu, H., Choi, M. S. & Kim, I. S. Fibronectin facilitates the invasion of Orientia tsutsugamushi into host cells through interaction with a 56-kDa type-specific antigen. *J Infect Dis* 198, 250-257 (2008).
29. Cho, B. A., Cho, N. H., Seong, S. Y., Choi, M. S. & Kim, I. S. Intracellular invasion by Orientia tsutsugamushi is mediated by integrin signaling and actin cytoskeleton rearrangements. *Infect Immun* 78, 1915-1923 (2010).
30. Ha, N. Y., Cho, N. H., Kim, Y. S., Choi, M. S. & Kim, I. S. An autotransporter protein from Orientia tsutsugamushi mediates adherence to nonphagocytic host cells. *Infect Immun* 79, 1718-1727 (2011).
31. Ko, Y., Choi, J. H., Ha, N. Y., Kim, I. S., Cho, N. H. & Choi, M. S. Active escape of Orientia tsutsugamushi from cellular autophagy. *Infect Immun* 81, 552-559 (2013).
32. Choi, J. H., Cheong, T. C., Ha, N. Y., Ko, Y., Cho, C. H., Jeon, J. H., So, I., Kim, I. K., Choi, M. S., Kim, I. S. & Cho, N. H. Orientia tsutsugamushi subverts dendritic cell functions by escaping from autophagy and impairing their migration. *PLoS Negl Trop Dis* 7, e1981 (2013).
33. Kim, S. W., Ihn, K. S., Han, S. H., Seong, S. Y., Kim, I. S. & Choi, M. S. Microtubule- and dynein-mediated movement of Orientia tsutsugamushi to the microtubule organizing center. *Infect Immun* 69, 494-500 (2001).
34. Lee, S. M., Kim, M. K., Kim, M. J. & Kang, J. S. Novel polysaccharide antigen of Orientia tsutsugamushi revealed by a monoclonal antibody. *FEMS Microbiol Lett* 297, 95-100 (2009).
35. Rikihisa, Y. & Ito, S. Localization of electron-dense tracers during entry of Rickettsia tsutsugamushi into polymorphonuclear leukocytes. *Infect Immun* 30, 231-243 (1980).
36. Kim, M. J., Kim, M. K. & Kang, J. S. Involvement of lipid rafts in the budding-like exit of Orientia tsutsugamushi. *Microb Pathog* 63C, 37-43 (2013).
37. Moree, M. F. & Hanson, B. Growth characteristics and proteins of plaque-purified strains of Rickettsia tsutsugamushi. *Infect Immun* 60, 3405-3415 (1992).
38. Persky, N. S., Ferullo, D. J., Cooper, D. L., Moore, H. R. & Lovett, S. T. The ObgE/CgtA GTPase influences the stringent response to amino acid starvation in Escherichia coli. *Mol Microbiol* 73, 253-266 (2009).
39. Jutras, B. L., Bowman, A., Brissette, C. A., Adams, C. A., Verma, A., Chenail, A. M. & Stevenson, B. EbfC (YbaB) is a new type of bacterial nucleoid-associated protein and

a global regulator of gene expression in the Lyme disease spirochete. *J Bacteriol* 194, 3395-3406 (2012).

40. Giengkam, S., Blakes, A., Utsahajit, P., Chaemchuen, S., Atwal, S., Blacksell, S. D., Paris, D. H., Day, N. P. & Salje, J. Improved Quantification, Propagation, Purification and Storage of the Obligate Intracellular Human Pathogen Orientia tsutsugamushi. *PLoS Negl Trop Dis* 9, e0004009 (2015).
41. Atwal, S., Giengkam, S., Jaiyen, Y., Feaga, H. A., Dworkin, J. & Salje, J. Clickable methionine as a universal probe for labelling intracellular bacteria. *J Microbiol Methods* 169, 105812 (2020).
42. Chibly, A. M., Querin, L., Harris, Z. & Limesand, K. H. Label-retaining cells in the adult murine salivary glands possess characteristics of adult progenitor cells. *PLoS One* 9, e107893 (2014).
43. Atwal, S., Giengkam, S., Chaemchuen, S., Dorling, J., Kosaisawe, N., VanNieuwenhze, M., Sampattavanich, S., Schumann, P. & Salje, J. Evidence for a peptidoglycan-like structure in Orientia tsutsugamushi. *Mol Microbiol* 105, 440-452 (2017).
44. Batty EM, C. S., Blacksell SB, Richards A, Paris D, Bowden R, Chan C, Lachumanan R, Day N, Donnelly P, Chen SL, Salje J. Long-read whole genome sequencing and comparative analysis of six strains of the human pathogen *Orientia tsutsugamushi. Plos Negl Trop Dis* (2018).
45. Beyer, A. R., VieBrock, L., Rodino, K. G., Miller, D. P., Tegels, B. K., Marconi, R. T. & Carlyon, J. A. Orientia tsutsugamushi Strain Ikeda Ankyrin Repeat-Containing Proteins Recruit SCF1 Ubiquitin Ligase Machinery via Poxvirus-Like F-box Motifs. *J Bacteriol* (2015).
46. Beyer, A. R., Rodino, K. G., VieBrock, L., Green, R. S., Tegels, B. K., Oliver, L. D., Marconi, R. T. & Carlyon, J. A. Orientia tsutsugamushi Ank9 is a multifunctional effector that utilizes a novel GRIP-like Golgi localization domain for Golgi-to-endoplasmic reticulum trafficking and interacts with host COPB2. *Cell Microbiol* (2017).
47. Evans, S. M., Rodino, K. G., Adcox, H. E. & Carlyon, J. A. Orientia tsutsugamushi uses two Ank effectors to modulate NF-κB p65 nuclear transport and inhibit NF-κB transcriptional activation. *PLoS Pathog* 14, e1007023 (2018).
48. VieBrock, L., Evans, S. M., Beyer, A. R., Larson, C. L., Beare, P. A., Ge, H., Singh, S., Rodino, K. G., Heinzen, R. A., Richards, A. L. & Carlyon, J. A. Orientia tsutsugamushi ankyrin repeat-containing protein family members are Type 1 secretion system substrates that traffic to the host cell endoplasmic reticulum. *Front Cell Infect Microbiol* 4, 186 (2014).
49. Yu, H. H. & Tan, M. Sigma28 RNA polymerase regulates hctB, a late developmental gene in Chlamydia. *Mol Microbiol* 50, 577-584 (2003).
50. Gunesekere, I. C., Kahler, C. M., Powell, D. R., Snyder, L. A., Saunders, N. J., Rood, J. I. & Davies, J. K. Comparison of the RpoH-dependent regulon and general stress response in Neisseria gonorrhoeae. *J Bacteriol* 188, 4769-4776 (2006).
51. Reniere, M. L., Whiteley, A. T., Hamilton, K. L., John, S. M., Lauer, P., Brennan, R. G. & Portnoy, D. A. Glutathione activates virulence gene expression of an intracellular pathogen. *Nature* 517, 170-173 (2015).
52. Portman, J. L., Dubensky, S. B., Peterson, B. N., Whiteley, A. T. & Portnoy, D. A. Activation of the *Listeria monocytogenes* Virulence Program by a Reducing Environment. *mBio* 8, (2017).
53. Sunyakumthorn, P., Bourchookarn, A., Pornwiroon, W., David, C., Barker, S. A. & Macaluso, K. R. Characterization and growth of polymorphic Rickettsia felis in a tick cell line. *Appl Environ Microbiol* 74, 3151-3158 (2008).
54. Ireton, K. Molecular mechanisms of cell-cell spread of intracellular bacterial pathogens. *Open Biol* 3, 130079 (2013).
55. Schindelin, J., Arganda-Carreras, I., Frise, E., Kaynig, V., Longair, M., Pietzsch, T., Preibisch, S., Rueden, C., Saalfeld, S., Schmid, B., Tinevez, J. Y., White, D. J.,

Hartenstein, V., Eliceiri, K., Tomancak, P. & Cardona, A. Fiji: an open-source platform for biological-image analysis. *Nat Methods* 9, 676-682 (2012).

56. Lee, S. H. Optimal integration of wide field illumination and holographic optical tweezers for multimodal microscopy with ultimate flexibility and versatility. *Opt Express* 26, 8049-8058 (2018).
57. Huang, B., Wang, W., Bates, M. & Zhuang, X. Three-dimensional super-resolution imaging by stochastic optical reconstruction microscopy. *Science* 319, 810-813 (2008).
58. Wang, Y., Schnitzbauer, J., Hu, Z., Li, X., Cheng, Y., Huang, Z. L. & Huang, B. Localization events-based sample drift correction for localization microscopy with redundant cross-correlation algorithm. *Opt Express* 22, 15982-15991 (2014).
59. Batish, M., Raj, A. & Tyagi, S. Single molecule imaging of RNA in situ. *Methods Mol Biol* 714, 3-13 (2011).

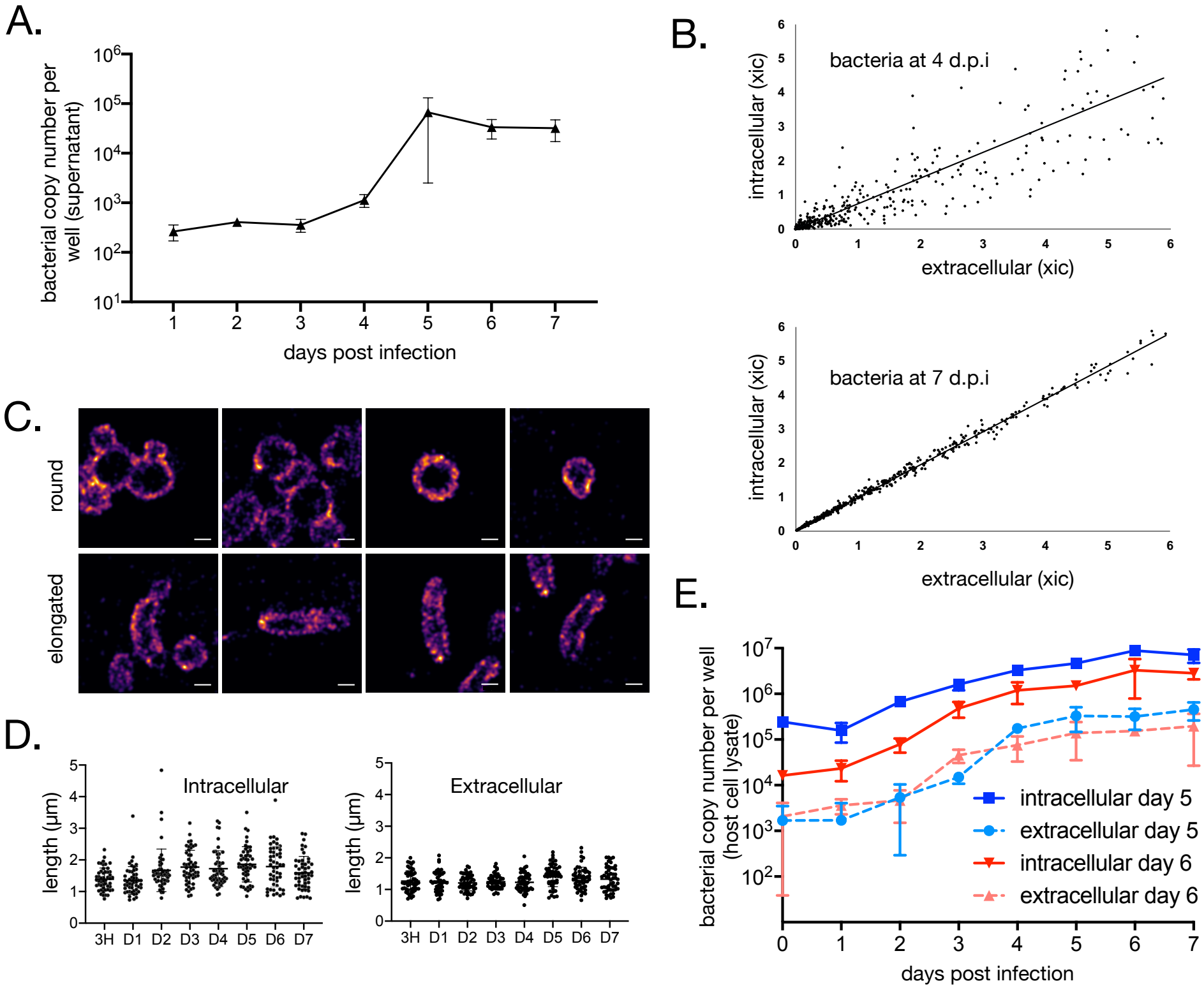

Figure 1. *Orientia tsutsugamushi* differentiates into a distinct extracellular state. A. Growth curve showing the exit of extracellular Ot into the culture supernatant of L929 cells. Bacteria were taken from the intracellular fraction after 6 days growth in L929 cells and used to inoculate fresh L929 cell cultures in 24 well plates. The total number of bacteria in the supernatant of each well was measured by using qPCR. B. Comparison of the mass spectrometry proteomic profiles (xic = extracted ion currents) of Ot isolated from the extracellular and intracellular populations 4 d.p.i. and 7 d.p.i. Correlation coefficients = 0.843 (4 d.p.i) and 1 (7 d.p.i). C. STORM images of intracellular Ot showing the round and elongated morphologies. Bacteria were labelled using an antibody against surface protein TSA56. Scale bar = 500 nm. D. Graphs showing Ot cell lengths at various times after infection as measured on confocal images. E. Growth curves showing the levels of intracellular Ot in L929 cells by measuring bacterial copy number in the cell lysates from one well of a 24 well plate up to 7 d.p.i. Intracellular and extracellular bacteria were recovered from infected L929 cells after 5 or 6 days of infection and used to infect fresh cultures of cells growing in 24-well plates. The growth curves show the number of bacteria in cell lysates from individual wells at various times up to 7 d.p.i.

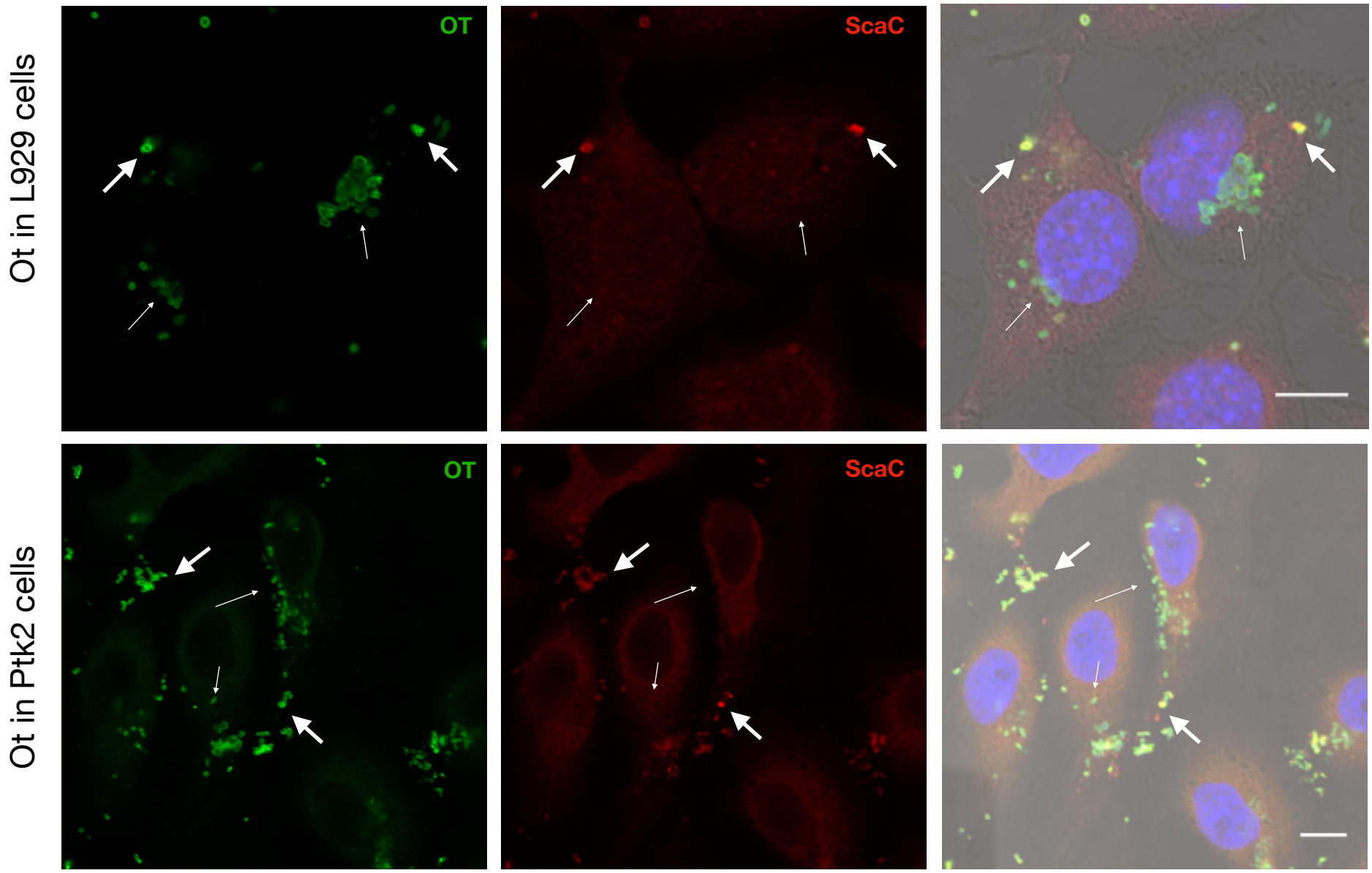

Figure 2. Surface protein ScaC is differentially expressed in Ot subpopulations and can be used to identify bacteria in the maturation stage of development. Confocal microscopy images showing Ot in L929 (top) and Ptk2 (bottom) cells. All images are taken 2 or 3 d.p.i. Bacteria were labelled using antibodies against surface proteins TSA56 (green) and ScaC (red) and a merged image including brightfield is shown in the third column. Additional images are shown in Supp. Fig. 7 and 8. Thick arrows indicate bacteria labelled with the ScaC antibody, thin arrows indicate bacteria not labelled with ScaC antibody. Scale bars = 10 µm.

Locus Tag	Gene ID	Gene name	Ratio (E/I)	Function
UT76-HP_02266	*nuoA*	NADH-quinone oxidoreductase subunit I	7.62	energy metabolism
UT76-HP_00279	*tpr3*	TPR repeat-containing protein 03	6.13	effectors and secretion systems
UT76-HP_01586		aplha/beta hydrolase	5.47	enzyme
UT76-HP_02172	*ybaB/ ebfC*	nucleoid-associated protein, YbaB/EbfC family	5.02	DNA binding, repair and replication
UT76-HP_01102	*spoT*	(p)ppGpp synthetase	4.99	dormany/stringent response/heat/ stress
UT76-HP_01915	*tpr8_1*	TPR repeat-containing protein 08	4.94	effectors and secretion systems
UT76-HP_01867	*murC*	UDP-N-acetylmuramate--L-alanine ligase	4.84	peptidoglycan
UT76-HP_00409	*nusB*	transcription antitermination factor NusB	4.56	RNA binding and processing
UT76-HP_00905		histidine phosphotransferase	4.34	signalling
UT76-HP_01844		intradiol ring-cleavage dioxygenase	3.69	oxidation-reduction processes
UT76-HP_01355		potassium transporter	3.47	transport
UT76-HP_01080		type IV secretion protein	3.28	effectors and secretion systems
UT76-HP_01602	*nuoD*	NADH-quinone oxidoreductase subunit D	3.26	energy metabolism
UT76-HP_00613	*rpoH*	RNA polymerase factor sigma-32	3.25	dormany/stringent response/heat/ stress
UT76-HP_01946	*xerD*	site-specific tyrosine recombinase XerD	3.25	DNA binding, repair and replication
UT76-HP_01601	*nuoc*	NADH-quinone oxidoreductase subunit C	3.11	energy metabolism
UT76-HP_01945	*virB6/*	conjugal transfer protein	3.09	effectors and secretion systems
UT76-HP_02056	*tpr8_2*	TPR repeat-containing protein 08	3.08	effectors and secretion systems
UT76-HP_01121		cytochrome b	2.98	energy metabolism
UT76-HP_00794		hypothetical protein	2.85	hypothetical protein
UT76-HP_01543		hybrid sensor histidine kinase/response regulator	2.84	signalling
UT76-HP_01097	*obgE*	GTPase ObgE	2.80	dormany/stringent response/heat/ stress
UT76-HP_02239	*idh*	isocitrate dehydrogenase, Idh	2.80	energy metabolism
UT76-HP_01254		hypothetical protein	2.76	hypothetical protein
UT76-HP_01589	*atpC*	ATP synthase subunit epsilon	2.60	energy metabolism
UT76-HP_00497	*dsbB*	disulfide bond formation protein B	2.54	oxidation-reduction processes
UT76-HP_01634	*parB*	chromosome partitioning protein	2.46	DNA binding, repair and replication
UT76-HP_02164	*rpmA*	50S ribosomal protein L27	2.46	protein synthesis
UT76-HP_00841	*rplX*	50S ribosomal protein L24	2.38	protein synthesis
UT76-HP_01490	*rbfA*	ribosome-binding factor A	2.38	protein synthesis
UT76-HP_01010	*fabI*	enoyl-ACP reductase	2.32	lipid and membrane
UT76-HP_01866		hypothetical protein	2.32	hypothetical protein
UT76-HP_00570	*aat*	aspartate aminotransferase	2.29	protein catabolic process
UT76-HP_01003	*murE*	UDP-N-acetylmuramoyl-L-alanyl-D-glutamate--2, 6-diaminopimelate ligase	2.27	peptidoglycan
UT76-HP_00817	*virB9*	P-type conjugative transfer protein VirB9	2.27	effectors and secretion systems
UT76-HP_00815	*ftsY*	signal recognition particle-docking protein FtsY	2.25	protein synthesis
UT76-HP_00510	*fmt*	methionyl-tRNA formyltransferase	2.23	protein synthesis
UT76-HP_00137	*efp*	elongation factor P	2.20	protein synthesis
UT76-HP_01888	*infC*	translation initiation factor IF-3	2.20	protein synthesis
UT76-HP_01762		conjugative transfer protein	2.20	effectors and secretion systems
UT76-HP_02013		acyl-[ACP]--phospholipid O-acyltransferase	2.07	lipid and membrane
UT76-HP_00136		extragenic suppressor protein SuhB	2.06	signalling
UT76-HP_00392	*rpiA*	ribose-5-phosphate isomerase	2.06	energy metabolism
UT76-HP_00820		thymidylate synthase (FAD)	2.06	other
UT76-HP_00448	*rph*	ribonuclease PH	2.05	protein synthesis
UT76-HP_00517	*fpr*	ferredoxin--NADP(+) reductase	2.05	oxidation-reduction processes
UT76-HP_01643	*mutS*	DNA mismatch repair protein MutS	2.03	DNA binding, repair and replication

Table 1. Summary of proteins upregulated in extracellular bacteria. Ot were isolated from the intracellular and extracellular fractions of infected L929 cells at 4 d.p.i. and their protein profiles were analyzed by shotgun proteomics. Proteins that were present at significantly elevated levels in the extracellular fraction compared with the intracellular fraction are shown here. The ratio of E/I shows the ratio of the means from three independent replicates from the extracellular (E) and intracellular (I) populations.

Locus Tag	Gene ID	Gene name	Ratio (I/E)	Function
UT76-HP_00965		RNA-binding protein	42.25	RNA binding and processing
UT76-HP_01100	*yccA*	membrane protein	34.91	protein synthesis
UT76-HP_01944	*surf1*	surfeit locus protein 1	12.99	energy metabolism
UT76-HP_02249	*ank1*	ankyrin repeat-containing protein 1	12.28	effectors and secretion systems
UT76-HP_01738	*prfA*	peptide chain release factor 1	8.33	protein synthesis
UT76-HP_00451	*rnpA*	ribonuclease P	7.72	RNA binding and processing
UT76-HP_00496	*ubiB*	ubiquinone biosynthesis protein UbiB	7.69	oxidation-reduction processes
UT76-HP_00730		ankyrin repeat-containing protein	6.89	transposase
UT76-HP_02120	*lpxK*	tetraacyldisaccharide 4'-kinase	6.68	lipid and membrane
UT76-HP_01600	*nuoB*	NADH-quinone oxidoreductase subunit B	6.62	oxidation-reduction processes
UT76-HP_00411	*gstA*	glutathione S-transferase	5.23	oxidation-reduction processes
UT76-HP_01955	*dapA*	4-hydroxy-tetrahydrodipicolinate synthase	5.21	protein synthesis
UT76-HP_01609		hypothetical protein	5.17	hypothetical
UT76-HP_01864	*glyQ*	glycine--tRNA ligase subunit alpha	4.98	protein synthesis
UT76-HP_00619	*ank13_1*	ankyrin repeat-containing protein 13	4.90	effectors and secretion systems
UT76-HP_01784	*ank13_2*	ankyrin repeat-containing protein 13	4.80	effectors and secretion systems
UT76-HP_01676	*atpF*	ATP synthase subunit b	4.21	energy metabolism
UT76-HP_00502	*apia*	triose-phosphate isomerase	4.12	energy metabolism
UT76-HP_02059		transposase	3.92	transposase
UT76-HP_01078		type IV secretion protein	3.72	effectors and secretion systems
UT76-HP_00501	*secG*	preprotein translocase subunit SecG	3.67	protein synthesis
UT76-HP_01119		hypothetical protein	3.40	hypothetical
UT76-HP_00981	*yihA*	YihA family ribosome biogenesis GTP-binding protein	3.34	protein synthesis
UT76-HP_00711		transposase	3.28	transposase
UT76-HP_00021		hypothetical protein	3.24	hypothetical
UT76-HP_02129		hypothetical protein	3.18	hypothetical
UT76-HP_01613		bifunctional 3-demethylubiquinone 3-O-methyltransferase/2-octaprenyl-6-hydroxy phenol methylase	3.14	other
UT76-HP_00477		hypothetical protein	2.89	hypothetical
UT76-HP_00792	*tlc*	ATP/ADP translocase; ADP,ATP carrier protein	2.89	energy metabolism
UT76-HP_01099		hypothetical protein	2.87	hypothetical
UT76-HP_01417	*der*	ribosome biogenesis GTPase Der	2.82	protein synthesis
UT76-HP_01006		16S rRNA methyltransferase	2.77	protein synthesis
UT76-HP_01560	*grxA*	glutaredoxin	2.74	oxidation-reduction processes
UT76-HP_00479		hypothetical protein	2.74	hypothetical
UT76-HP_01485	*ubiB*	ubiquinone biosynthesis protein UbiB	2.59	oxidation-reduction processes
UT76-HP_00403		thiol:disulfide interchange protein	2.56	oxidation-reduction processes
UT76-HP_00614		hypothetical protein	2.56	hypothetical
UT76-HP_02138	*pipB2*	Secreted effector protein PipB2	2.54	effectors and secretion systems
UT76-HP_02016	*rnc*	ribonuclease III	2.51	RNA binding and processing
UT76-HP_01577		ATPase	2.48	other
UT76-HP_00779	*hscB*	co-chaperone HscB	2.46	protein synthesis
UT76-HP_01644	*secF*	protein translocase subunit SecF	2.42	protein synthesis
UT76-HP_00429		conjugal transfer protein	2.41	effectors and secretion systems
UT76-HP_01419	*panF*	sodium:pantothenate symporter	2.40	other
UT76-HP_01604	*nuoF*	NADH-quinone oxidoreductase subunit F	2.31	oxidation-reduction processes
UT76-HP_01731		hypothetical protein	2.29	hypothetical
UT76-HP_00149		ATP-binding protein	2.28	other
UT76-HP_01729	*tsaD*	tRNA (adenosine(37)-N6)-threonylcarbamoyltransferase	2.26	other
UT76-HP_00401	*ccm*	heme exporter protein C	2.25	other
UT76-HP_00449		cytochrome c	2.25	energy metabolism
UT76-HP_02098	*recR*	recombination protein RecR	2.24	DNA binding, repair and replication
UT76-HP_00040	*nrdB*	ribonucleotide-diphosphate reductase subunit beta, NrdB	2.21	DNA binding, repair and replication
UT76-HP_00431		cytochrome c oxidase subunit II	2.17	energy metabolism
UT76-HP_00783		aminotransferase class V-fold PLP-dependent enzyme	2.15	other
UT76-HP_02272	*tilS*	tRNA lysidine(34) synthetase TilS	2.13	protein synthesis
UT76-HP_01559		hypothetical protein	2.08	hypothetical
UT76-HP_00543		hypothetical protein	2.07	hypothetical
UT76-HP_01551		hypothetical protein	2.06	hypothetical
UT76-HP_00487	*ubiH*	2-polyprenyl-6-methoxyphenol 4-hydroxylase	2.04	oxidation-reduction processes
UT76-HP_00512	*rimM*	ribosome maturation factor RimM	2.03	protein synthesis

Table 2. Summary of proteins upregulated in intracellular bacteria. Ot were isolated from the intracellular and extracellular fractions of infected L929 cells at 4 d.p.i. and their protein profiles were analyzed by shotgun proteomics. Proteins that were present at significantly elevated levels in the intracellular fraction compared with the extracellular fraction are shown here. The ratio of E/I shows the ratio of the means from three independent replicates from the extracellular (E) and intracellular (I) populations.

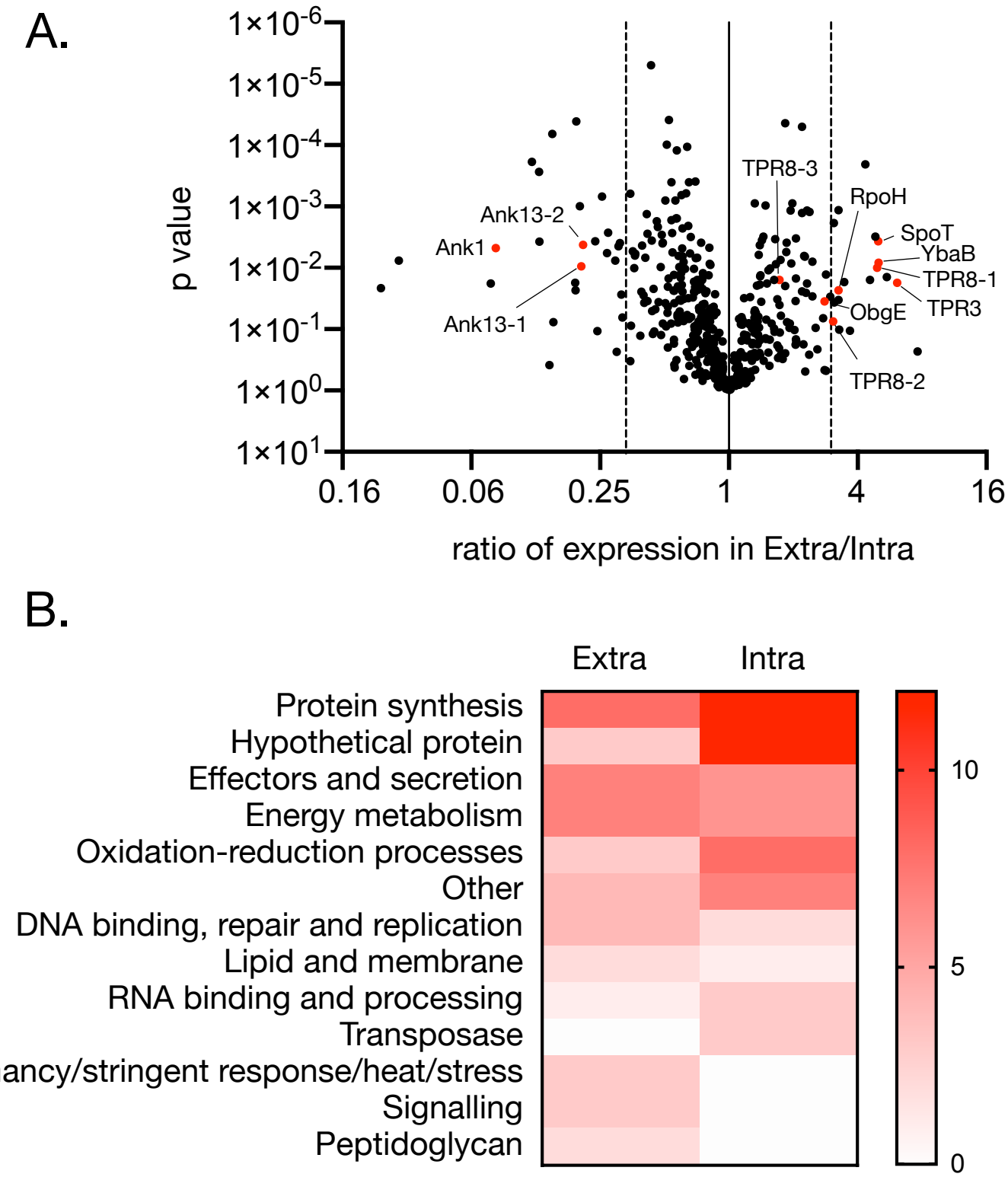

Figure 3. Differential protein expression in intracellular and extracellular fractions. A. Volcano plot showing the ratio of expression between extracellular and intracellular fractions for individual proteins and the p value for each data point, based on the mean normalized label-free quantification value from three independent replicates. Genes mentioned in the text are highlighted. B. Heatmap showing differential expression of different classes of genes in the extracellular or intracellular bacteria. The number of genes in each category that were significantly enriched in one fraction over the other, as detailed in Tables 1 and 2, are indicated.

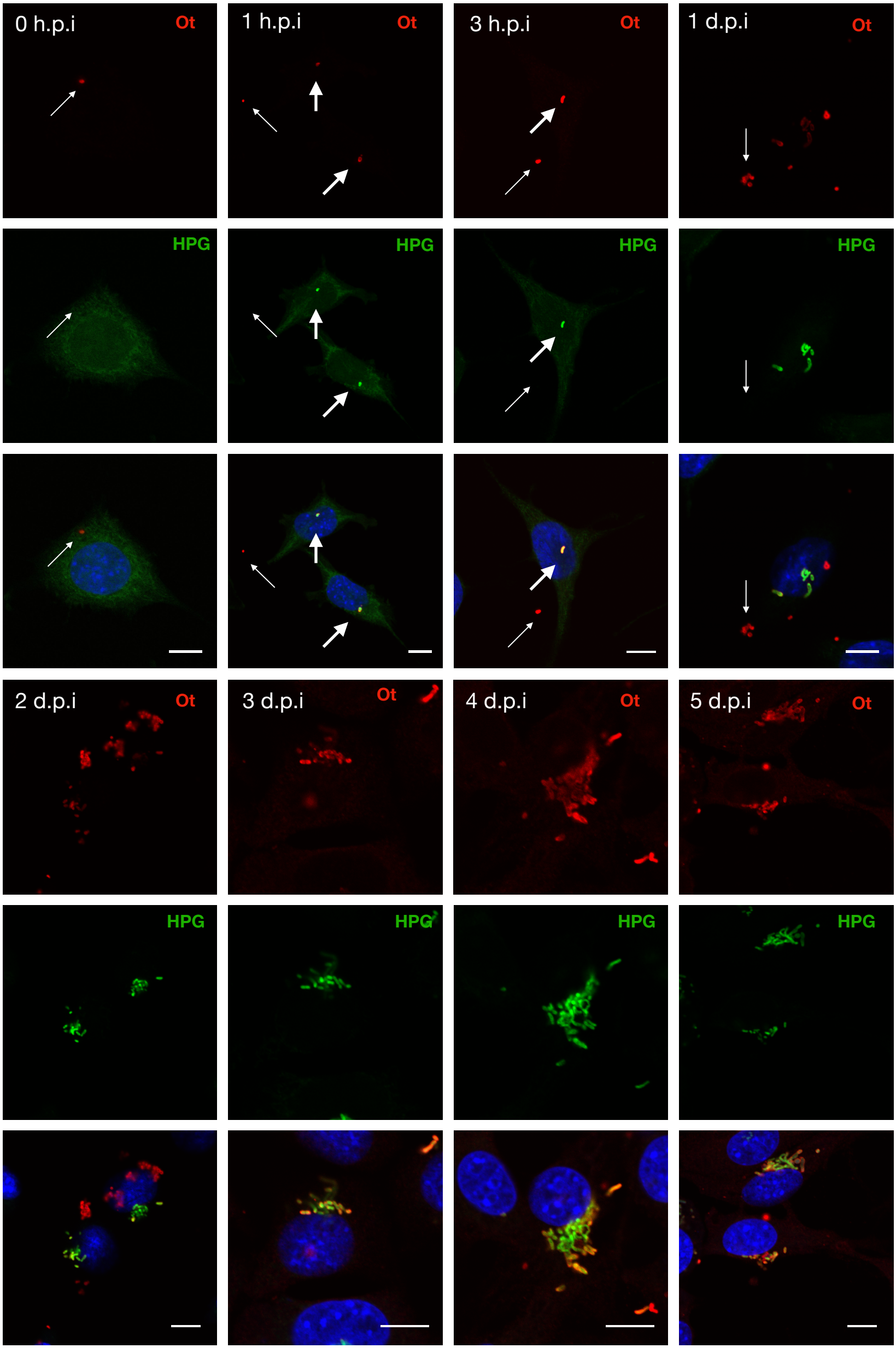

Figure 4. Ot becomes metabolically active shortly after entry into host cells. A clickable methionine probe (HPG, green, middle panels) was used to identify metabolically active bacteria growing in L929 cells over the course of 5 days of infection (0 h.p.i. to 7 d.p.i.). All bacteria were counterstained with a TSA56 antibody (Ot, red, top panels). Merged images including a DAPI DNA stain (blue) are shown in the bottom panels. Thick arrows indicate metabolically active (HPG-positive) bacteria, thin arrows indicate metabolically inactive (HPG-negative) bacteria. Scale bars = 10 µm.

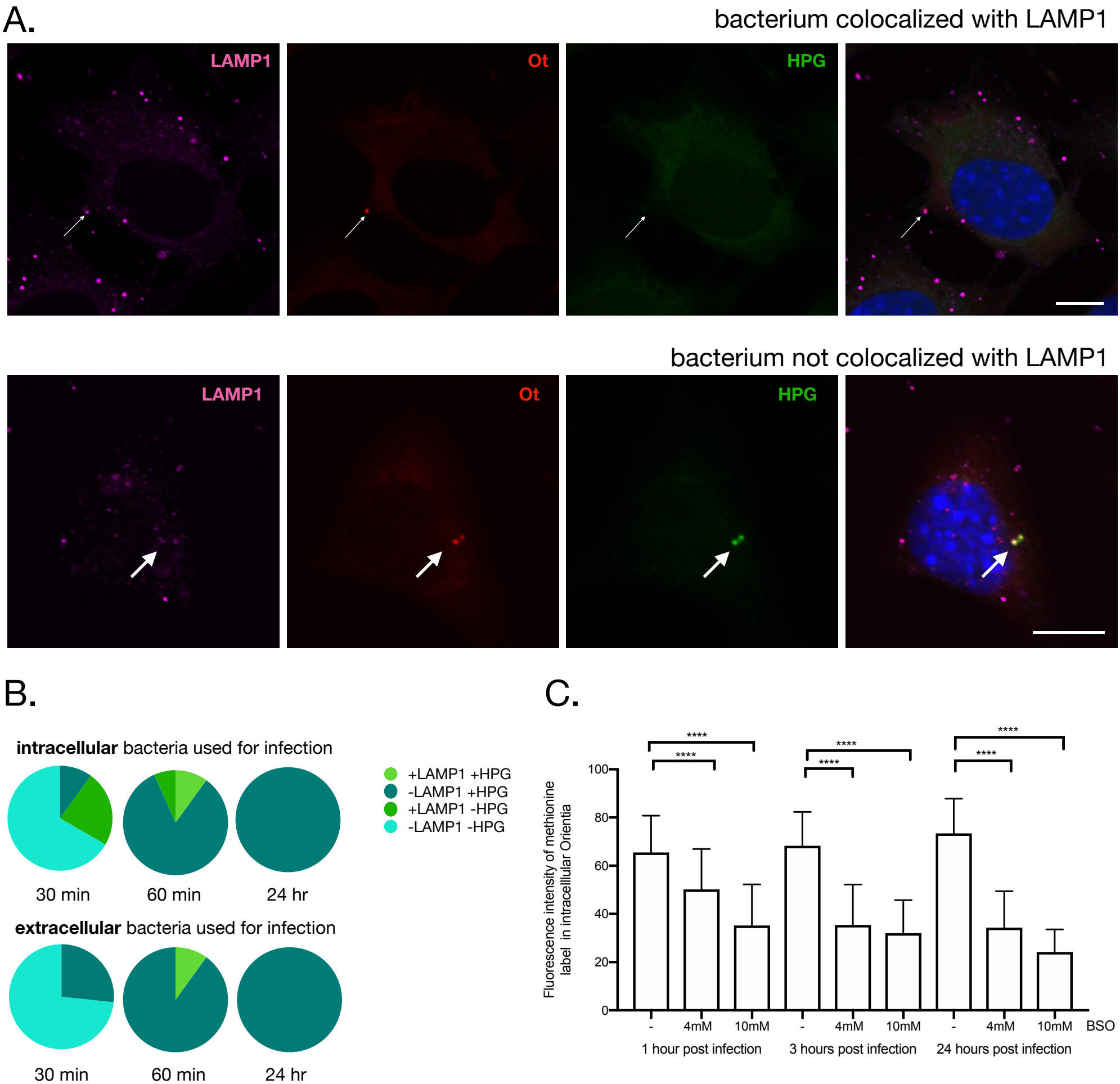

Figure 5. Ot becomes metabolically active shortly after entry and this is regulated by the host cell redox status. A. Representative confocal microscopy images of intracellular Ot 30-60 mins post infection, showing an example of a bacterium that does (top) and does not (bottom panel) colocalize with LAMP1. Late endosomes are labelled with LAMP1 (magenta), Ot is counterstained with 16S RNA FISH probes (red), and metabolic activity is measured with a clickable methionine probe (HPG, green). B. Quantification of confocal data, measuring the fraction of all bacteria (measured by the presence of 16S RNA FISH labelling) that colocalize with LAMP1 and HPG after 30 mins, 60 mins and 24 hours in cells infected with bacteria from intracellular (top) or extracellular (bottom) populations. Thirty bacteria were quantified at each time point. C. Decreased levels of reduced glutathione in L929 cell cytoplasm, induced by treatment with buthionine sulfoximine (BSO), lead to reduced metabolic activity in Ot. The fluorescence intensity of HPG-labelled bacteria in confocal microscopy images was quantified at 1, 3 and 24 h.p.i. and in the presence of 0, 4 mM or 10 mM BSO. 100 individual bacteria were measured in each condition.

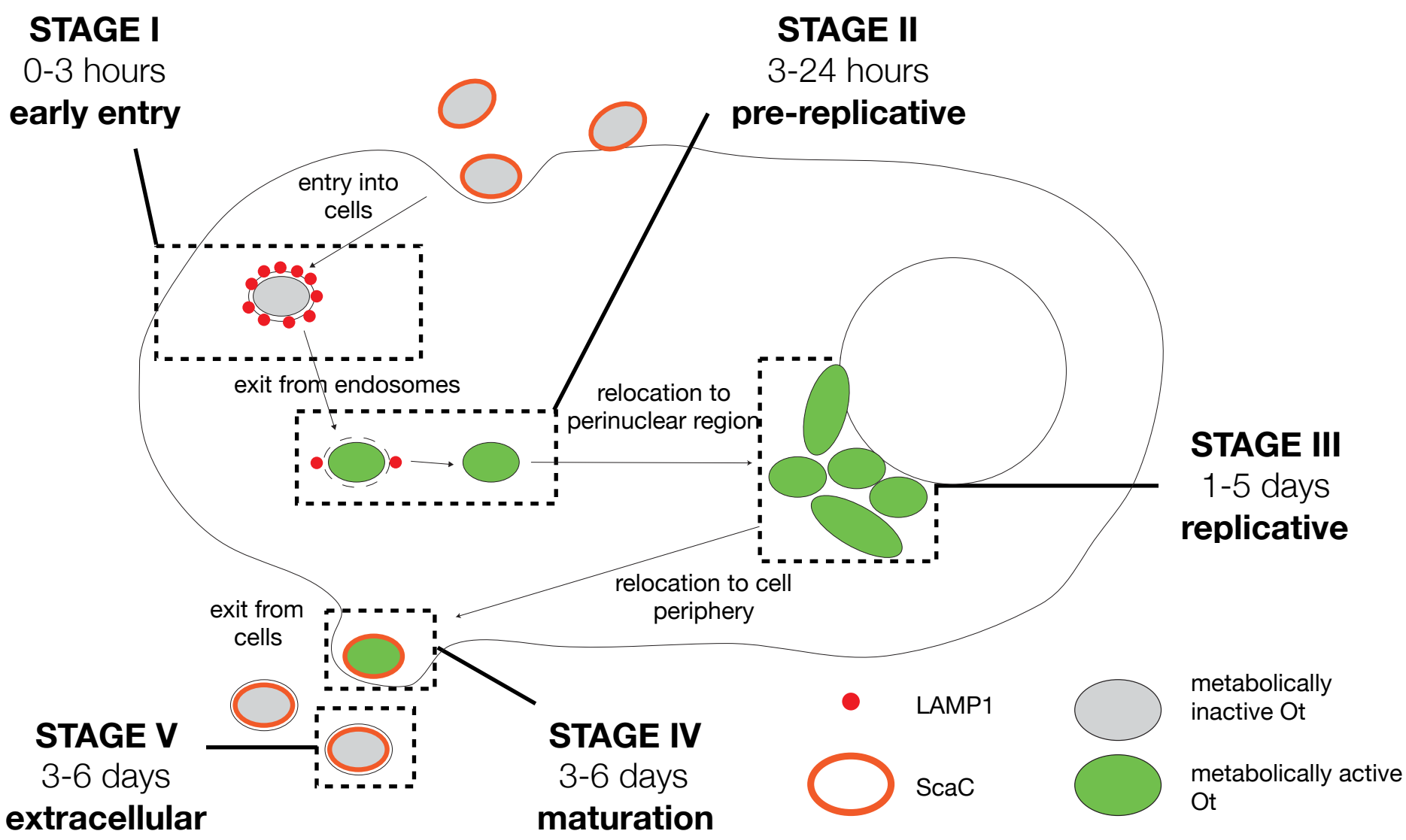

Stage	Name	Time	Protein synthesis?	DNA synthesis?	Location	Infectious?
I	Early entry	0-3 hours	NO	NO	intra	?
II	Pre-replicative	3-24 hours	YES	NO	intra	?
III	Replicative	1-5 days	YES	YES	intra	YES
IV	Maturation	3-6 days	YES	?	intra	
V	Extracellular	3-6 days	NO	NO	extra	YES

Figure 6. An overview of the distinct stages in the intracellular lifecycle of Ot. Details and timings reflect measurements for OT strain UT76 growing in L929 cells.